Applied Physics Letters ACCEPTED MANUSCRIPT

This is the author's peer reviewed, accepted manuscript. However, the online version of record will be different from this version once it has been copyedited and typeset.

PLEASE CITE THIS ARTICLE AS DOI: 10.1063/5.0102088

AIP Publishing

Low Thermal Conductivity in A-site High Entropy Perovskite Relaxor Ferroelectric

Wei Xiong[a,b], Hangfeng Zhang[b,], Zimeng Hu[b], Michael J Reece[b], Haixue Yan[b,*]*

a. Light Alloy Research Institute, Central South University, Changsha, 410083, China

b. School of Engineering and Materials Science, Queen Mary University of London, Mile End Road, London E1 4NS, UK.

*Corresponding authors.

Email addresses: hangfeng.zhang@qmul.ac.uk (H. Zhang); h.x.yan@qmul.ac.uk (H. Yan)

ABSTRACT

A-site disordered high entropy perovskite $(Pb_{1/6}Ba_{1/6}Sr_{1/6}Ca_{1/6}Na_{1/6}Bi_{1/6})TiO_3$ (PBSCNBi) ceramic was prepared by a solid-state reaction method. XRD and SEM-EDX confirmed a single-phase tetragonal solid solution. Dielectric and hysteresis loop measurements showed relaxor ferroelectricity at room temperature; Curie Weiss fitting gives a Burns temperature (T_b) of 123℃，and Vogel-Fulcher fitting gives a freezing temperature (T_f) of -67.24 ℃，which confirms the room-temperature relaxor ferroelectricity of PBSCNBi. This is attributed to local chemical inhomogeneities in the high entropy ceramics. PBSCNBi also has a low thermal conductivity (1.15 $Wm^{-1}K^{-1}$ at room temperature) compared to all of its constituent simple perovskites (e.g $BaTiO_3$, $PbTiO_3$, $SrTiO_3$ $CaTiO_3$ and $Na_{1/2}Bi_{1/2}TiO_3$ in the range of 25℃ to 100℃), which is attributed to the enhanced phonon scattering by both polar nanoregions (PNRs) and the mass contrast effect in the multi-element perovskite. This work demonstrates the great potential of making A-site high entropy ceramics with relaxor ferroelectric properties.

High entropy ceramics have been increasingly reported in recent years, and a range

Applied Physics Letters ACCEPTED MANUSCRIPT
This is the author's peer reviewed, accepted manuscript. However, the online version of record will be different from this version once it has been copyedited and typeset.
PLEASE CITE THIS ARTICLE AS DOI: 10.1063/5.0102088
AIP Publishing

of systems incorporating high entropy design have been synthesised, such as rock-salt metal oxides[1-4], fluorites[5-7], bismuth layer-structured ferroelectric (BLSFs)[8, 9] and perovskites[10-13]. Because of the good synthesisability and vast compositional space of high entropy ceramics, there is considerable potential to fabricate compositions with useful properties. This makes high entropy ceramics popular candidates for many applications, including thermoelectric[14-16], electrochemical[2, 3, 11], thermal insulation[5, 12] and energy storage[13, 17].

Owing to their unique ABO_3 structure, high entropy perovskites provide a very interesting system to explore for ferroelectric and dielectric materials. However, studies on the ferroelectric/dielectric properties of high entropy perovskites are scarce. Moreover, for high entropy ceramics, the difference in size and electronegativity between the constituent cations are generally greater than that of transition metal elements in high entropy alloys. This large difference in the chemical characteristics of the cations could potentially promote the formation of local chemical inhomogeneities and produce relaxor ferroelectricity. In our previous work[18], we made an A-site disordered high entropy perovskite $(Pb_{0.25}Ba_{0.25}Sr_{0.25}Ca_{0.25})TiO_3$ (PBSC) ceramic, including a small amount (undetectable by XRD) of a non-ferroelectric secondary phase, and demonstrated that it has relaxor-like behaviour. We identified the compositional fluctuations that led to the coexistence of long-range ordered ferroelectric domains and short-range ordered relaxor ferroelectric regions in the PBSC system, which was confirmed by high-resolution scanning transmission electron microscope (HR-STEM) images and ferroelectric hysteresis loop measurements. A few other papers on high

Applied Physics Letters ACCEPTED MANUSCRIPT
This is the author's peer reviewed, accepted manuscript. However, the online version of record will be different from this version once it has been copyedited and typeset.
PLEASE CITE THIS ARTICLE AS DOI: 10.1063/5.0102088
AIP Publishing

entropy perovskites have also highlighted high entropy effects, inducing relaxor behaviour[8, 19, 20]. In this work, we add sodium (Na) and bismuth (Bi) into the PBSC model system to make a single phase high entropy perovskite $(Pb_{1/6}Ba_{1/6}Sr_{1/6}Ca_{1/6}Na_{1/6}Bi_{1/6})TiO_3$ (PBSCNBi) The extra components of PBSCNBi could produce a stronger compositional fluctuation than in PBSC and enhance the relaxor behaviour, moreover, the Na-Bi pair is known to facilitate relaxor ferroelectricity, as in $Na_{1/2}Bi_{1/2}TiO_3$-$BaTiO_3$ (NBT-BT) and other solid solutions[21-23]. Our results demonstrate that PBSCNBi is a single phase displacive-type relaxor ferroelectric material, and its relaxor ferroelectricity is indeed enhanced by the addition of Na and Bi compared to PBSC.

Additionally, some groups[24, 25] have demonstrated the effective tuning of thermal conductivity by ferroelectric domain wall engineering; the dimensions of the spacing of these ferroelectric domain structures can be reduced to ~100 nm and thus contribute to phonon scattering. This is usually done by fabricating ferroelectric thin films[24-26]. In this regard, using relaxor ferroelectrics should also be effective in reducing thermal conductivity as they possess polar structures of only a few nanometres (polar nanoregions, PNRs), which is less than the mean free path of phonons and therefore could contribute to a reduction in thermal conductivity. Studies on the thermophysical properties of relaxor ferroelectrics are scarce. Here we demonstrate that PBSCNBi has a lower thermal conductivity than PBSC and all of the constituent simple perovskites, which could be attributed to the combined effects of strong mass contrast and PNRs. This provides a hierarchical approach to designing low-thermal-conductivity materials

Applied Physics Letters ACCEPTED MANUSCRIPT
This is the author's peer reviewed, accepted manuscript. However, the online version of record will be different from this version once it has been copyedited and typeset.
PLEASE CITE THIS ARTICLE AS DOI: 10.1063/5.0102088

for thermoelectric applications.

The high entropy ceramic PBSCNBi was synthesised by a solid-state reaction method (see supplementary material). Its XRD pattern (**Figure 1**) shows that PBSCNBi has a tetragonal structure (*P*4*mm*, $a = b = 3.9103(2)$ Å; $c = 3.9183(3)$ Å, see supplementary information for details of refinement). Note that the (002) and (200) peaks show a slight asymmetric peak at around 46.5° 2θ that is barely distinguishable, which is consistent with the small degree of tetragonality (c/a = 1.002). EDX analysis (**Table S1**) of a representative fracture surface of the PBSCNBi ceramic (**Figure S1**) shows a generally homogeneous distribution of elements in the correct atomic ratios. Additional EDX of a polished flat surface of the ceramic shows slight segregation of Ba and Bi at the grain boundaries, see **Figure S2**). Compared to the four-component composition PBSC in the previous work[18], which had a secondary phase identified by SEM-EDX in both the matrix and grain boundaries, the better single-phase formation of PBSCNBi is attributed to enhanced entropy-driven phase stabilization as more components produces a higher configurational entropy.

Applied Physics Letters ACCEPTED MANUSCRIPT
This is the author's peer reviewed, accepted manuscript. However, the online version of record will be different from this version once it has been copyedited and typeset.
PLEASE CITE THIS ARTICLE AS DOI: 10.1063/5.0102088
AIP Publishing

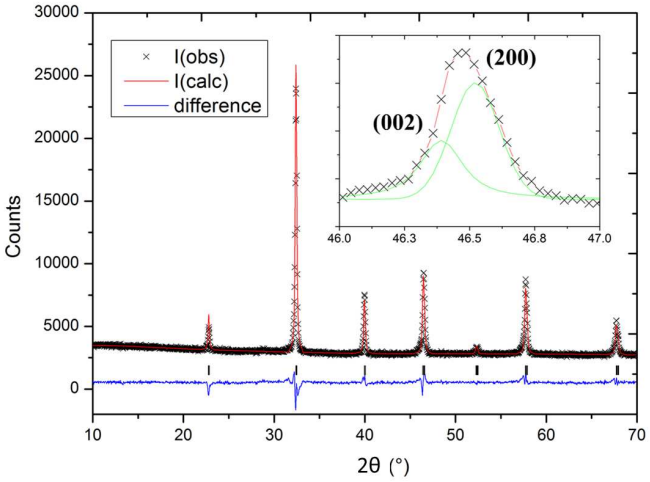

Figure 1. Rietveld refinement[27] of XRD pattern of $(Pb_{1/6}Ba_{1/6}Sr_{1/6}Ca_{1/6}Na_{1/6}Bi_{1/6})TiO_3$ (PBSCNBi) using FullProf software[28], the inset shows the peak deconvolution at around 46.5° 2θ using Voigt fitting, corresponding to the (002) and (200) reflections.

Figure 2a shows the temperature-dependent dielectric permittivity (ε') and loss tanδ of PBSCNBi. The results show apparent frequency dispersion of the dielectric peaks, indicating that the material is a relaxor ferroelectric. The dielectric permittivity data at 100kHz was fitted to the Curie-Weiss law[29] (**Figure 2b**):

$$\varepsilon' = \frac{C}{T - \theta} \qquad \text{Eq. (1)}$$

Where ε' is the dielectric permittivity, C the Curie constant, T the absolute temperature and θ the Curie-Weiss temperature. The fitting gives a Curie-Weiss temperature of -103℃, and a Curie constant of around 7.6 x 10^5℃, which is slightly higher than that of PBSC in our previous work (3.97 x 10^5℃)[18]. The value is of the

Applied Physics Letters ACCEPTED MANUSCRIPT
This is the author's peer reviewed, accepted manuscript. However, the online version of record will be different from this version once it has been copyedited and typeset.
PLEASE CITE THIS ARTICLE AS DOI: 10.1063/5.0102088
AIP Publishing

order of 10^5℃, which indicates that PBSCNBi is a displacive type ferroelectric[30]. The displacive type ferroelectric nature of PBSCNBi is interesting as high entropy materials usually have a disordered distribution of different elements (as shown in **Figure S1**), and one would not expect a totally disordered system to show displacive-type ferroelectricity, which suggests that local compositional variation coexists with the displacement of ions in the PBSCNBi lattice. We have also extrapolated the Burns temperature (T_b) from the real part of the permittivity data to be 123℃ according to the Curie-Weiss fitting (**Figure 2b**). The imaginary part of permittivity data (**Figure 2c**) was fitted to the Vogel-Fulcher relation[31] (**Figure 2d):**

$$f = f_0 e^{-\frac{E_a}{k(T_m - T_f)}} \quad \text{Eq. (2)}$$

Where f_0 is the attempt frequency, E_a the activation energy, k the Boltzmann constant, T_m the temperature corresponding to the maximum of the imaginary part of the permittivity and T_f the freezing temperature. Fitting gives a T_f of -67.24℃, E_a of 0.20 eV and f_0 of around 10^{13} Hz. The freezing temperature (-67.24℃) is well below room temperature and the Burns temperature (123℃), which is consistent with the observed room temperature relaxor behaviour (frequency dispersion) (**Figure 2a**).

Applied Physics Letters ACCEPTED MANUSCRIPT
This is the author's peer reviewed, accepted manuscript. However, the online version of record will be different from this version once it has been copyedited and typeset.
PLEASE CITE THIS ARTICLE AS DOI: 10.1063/5.0102088
AIP Publishing

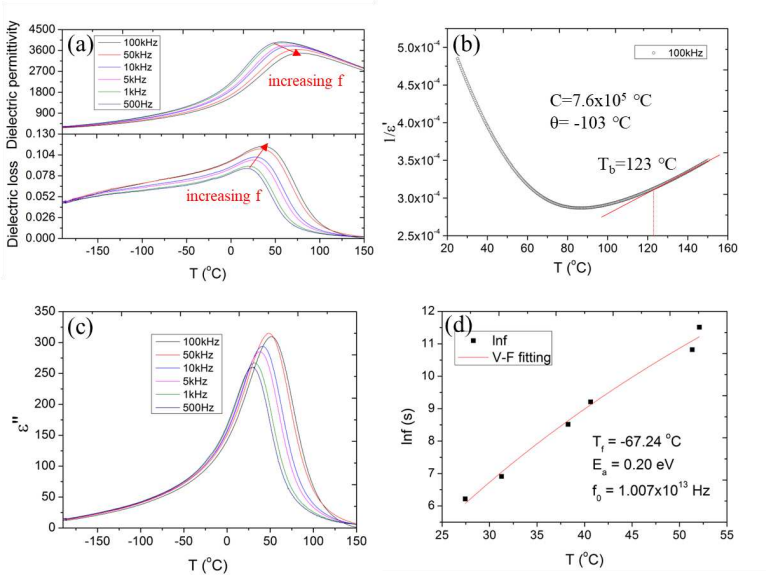

Figure 2. (a) Temperature-dependent dielectric permittivity and loss of PBSCNBi; (b) Curie-Weiss fitting on the dielectric permittivity of PBSCNBi at 100kHz; (c) Imaginary part of permittivity of PBSCNBi; (d) Vogel-Fulcher fitting on the imaginary part of permittivity data of PBSCNBi.

Applied Physics Letters ACCEPTED MANUSCRIPT
This is the author's peer reviewed, accepted manuscript. However, the online version of record will be different from this version once it has been copyedited and typeset.
PLEASE CITE THIS ARTICLE AS DOI: 10.1063/5.0102088
AIP Publishing

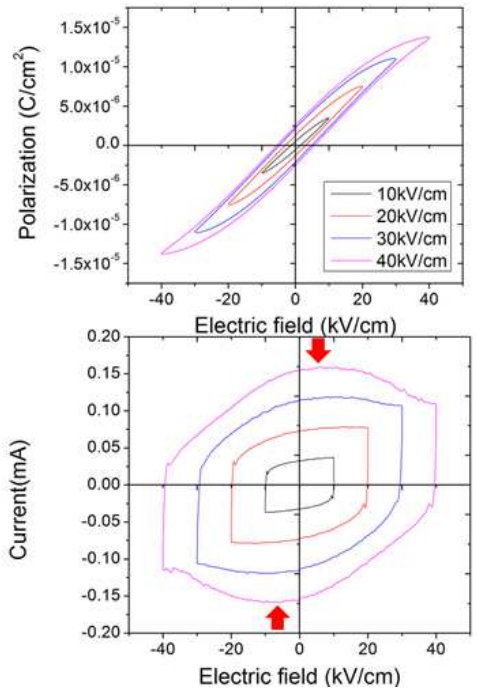

Figure 3. (a) P-E and (b) I-E hysteresis loops of PBSCNBi at room temperature, red arrows indicate the near-zero-field current peak, corresponding to the polar nanoregions.

Figure 3 presents the P-E and I-E hysteresis loops of PBSCNBi at room temperature. On cooling, at the Burns temperature (123℃), polar nanoregions nucleate and grow as the temperature decreases (ergodic state) until reaching the freezing temperature (-67.24℃), where they become "frozen" due to enhanced correlation and enter a nonergodic state. In this state, an applied electric field will irreversibly transform the relaxor ferroelectric into a normal ferroelectric. The observed reversible current peaks at near zero-field（marked by red arrows）at room temperature are a clear indication of an ergodic relaxor state and the existence of polar nanoregions, which is

Applied Physics Letters ACCEPTED MANUSCRIPT
This is the author's peer reviewed, accepted manuscript. However, the online version of record will be different from this version once it has been copyedited and typeset.
PLEASE CITE THIS ARTICLE AS DOI: 10.1063/5.0102088
AIP Publishing

consistent with the dielectric permittivity data, and supports the hypothesis that local inhomogeneity coexists with an overall homogeneous and disordered composition in the high entropy perovskite. A recent paper[32] on $Ba_{0.6}Sr_{0.4}TiO_3$ (BST) directly observed that local heterogeneity and global homogeneity coexist, with polar nanoregions in the range of 2-4 nm; Other studies of BST-based and $Na_{1/2}Bi_{1/2}TiO_3$ (NBT)-based systems also showed that the materials have polar nanoregions embedded in a non-polar matrix[33-35]. In contrast to these relaxor ferroelectrics, our PBSCNBi has a polar structure (P4mm) at room temperature and shows much stronger frequency dispersion, indicating that PBSCNBi probably has a high concentration of polar nanoregions. By analogy to the solid solutions and intermetallic phases in high entropy alloys, when the number of atom species (e.g. 6 cations in the A-site of PBSCNBi) exceeds the number of corresponding sublattice sites (1 for A-site of a ABO_3 perovskite structure), intermetallic local structures have an enhanced configurational entropy and can co-exist within a disordered solid solution in a multi-component system[36]. Such short-range ordered structures have been commonly observed in other medium-to-high entropy compositions.[37-40] In the context of high entropy relaxor ferroelectric perovskites, local chemical inhomogeneities (local polar structure) are also likely to be stabilized and co-exist within a homogeneous matrix (weak polar structure related to displacement of ions, which is supported by XRD data and Curie constant). This implies that high entropy materials like PBSCNBi probably produce relaxor behaviour by a slightly different mechanism to normal solid solutions; in the sense that besides the relaxor behaviour introduced by charge disorder (e.g. $Pb(Mg, Nb)O_3$) and lattice distortion (e.g.

Applied Physics Letters ACCEPTED MANUSCRIPT
This is the author's peer reviewed, accepted manuscript. However, the online version of record will be different from this version once it has been copyedited and typeset.
PLEASE CITE THIS ARTICLE AS DOI: 10.1063/5.0102088
AIP Publishing

Ba(Zr, Ti)O_3), high configurational entropy itself could also stabilizes local chemical inhomogeneities that give rise to the short-range ordered polar nanoregions. It is notable that the relaxor behaviour is also more apparent in PBSCNBi than in PBSC (e.g. enhanced frequency dispersion and increased diffusivity, $\gamma_{\mathrm{PBSCNBi}} = 1.74 > \gamma_{\mathrm{PBSC}} = 1.36$), which probably indicates a higher degree of local chemical inhomogeneity in PBSCNBi. Considering that the configurational entropy (S_{config}) of PBSCNBi (1.79R) is higher than that of PBSC (1.38R), this suggests that the effect of high entropy design in promoting local chemical inhomogeneity and relaxor ferroelectricity probably have a threshold entropy value, below which the effect is much reduced.

Another merit of a highly disordered multi-component structures is reduced thermal conductivity. **Figure 4** presents the thermal conductivity of PBSCNBi from room temperature to 400℃ (see supplementary information for uncertainty analysis). PBSCNBi has a lower thermal conductivity (1.29 $Wm^{-1}K^{-1}$ at 100℃) compared to the other A-site disordered high entropy perovskite PBSC (2.65 $Wm^{-1}K^{-1}$ at 100℃) and all of the constituent simple perovskites[41-45] (2.4 To 7.5 $Wm^{-1}K^{-1}$ at 100℃) and is temperature-independent. The temperature dependencies of thermal conductivities of PBSCNBi and PBSC deviate from the normal T^{-1} Umklapp behaviour due to the greatly enhanced mass scattering of phonons in multi-component systems[46], which is characterized by $\tau_m^{-1} = V\Gamma\omega^4/4\pi v^3$,[47] where V is the defect volume (i.e. considering an atom of different mass as defect site), v the sound velocity, ω the angular frequency, $\Gamma = \sum_{i=1}^{n} x_i(\frac{m_i-\bar{m}}{\bar{m}})^2$ is the mass variance where m_i and x_i are the mass and concentration of the ith component, respectively, and $\bar{m}$ is the average mass of all of

Applied Physics Letters ACCEPTED MANUSCRIPT
This is the author's peer reviewed, accepted manuscript. However, the online version of record will be different from this version once it has been copyedited and typeset.
PLEASE CITE THIS ARTICLE AS DOI: 10.1063/5.0102088
AIP Publishing

the components. Note that PBSC has weaker relaxor ferroelectricity and lower configurational entropy than PBSCNBi. The reduced thermal conductivity of PBSCNBi compared to the PBSC can be attributed to two factors, one is the large lattice distortion caused by the size and mass mismatch of the constituent elements (**Table 1**), which act as phonon scattering sites. Additionally, polar nanoregions could also contribute the reduction in thermal conductivity; the nanoscale inhomogeneities have different elastic properties to the matrix, and this mismatch at their interface produces enhanced phonon scattering[48]. The combined effects of polar nanoregions and large mass and size contrast is responsible for the low thermal conductivity of high entropy perovskite PBSCNBi.

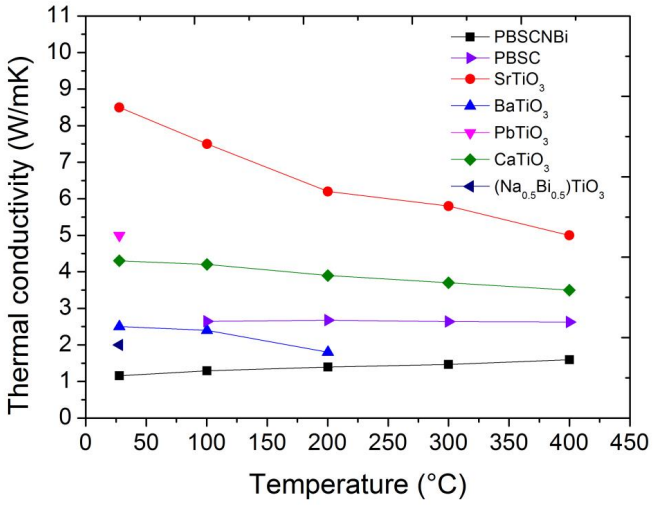

Figure 4. Temperature dependencies of thermal conductivities of high entropy perovskite PBSCNBi, PBSC and other simple perovskites[41-45].

Applied Physics Letters ACCEPTED MANUSCRIPT
This is the author's peer reviewed, accepted manuscript. However, the online version of record will be different from this version once it has been copyedited and typeset.
PLEASE CITE THIS ARTICLE AS DOI: 10.1063/5.0102088
AIP Publishing

Table 1. Ionic radius and atomic mass of elements of PBSCNBi.

	Pb	**Ba**	**Sr**	**Ca**	**Na**
Radius(pm)	149.0	161.0	144.0	134.0	139.0
Mass	207.200	137.327	87.620	40.078	22.990
	Bi	**Ti**	**O**	**Mean**	**σ**
Radius(pm)	117.0	60.5	140.0	130.6	29.0
Mass	208.980	47.867	15.999	96.008	74.232

In conclusion, an A-site high entropy perovskite $(Pb_{1/6}Ba_{1/6}Sr_{1/6}Ca_{1/6}Na_{1/6}Bi_{1/6})TiO_3$ (PBSCNBi) with tetragonal structure was synthesised by a solid-state reaction and sintering processing route. XRD and SEM-EDX confirmed that it has a long range homogeneous single-phase composition. However, apparent frequency dispersion of the permittivity data and the near-zero-field current peaks in the P-E loops suggest that local inhomogeneities exist, resulting in relaxor ferroelectric behaviour of the material, which is consistent with the Curie-Weiss fitting results that shows PBSCNBi is a displacive-type relaxor ferroelectric despite its disordered global structure. PBSCNBi has a freezing temperature (T_f) of -67.24℃ and Burns temperature (T_b) of 123℃, further supporting its room-temperature relaxor behaviour is related to polar nanoregions. PBSCNBi has a lower thermal conductivity than all its constituent simple perovskites, which can be attributed to the combined effect of polar nanoregions and large atomic size and mass contrast.

Supplementary Material

See supplementary information for experimental methods, uncertainty analysis,

Applied Physics Letters ACCEPTED MANUSCRIPT
This is the author's peer reviewed, accepted manuscript. However, the online version of record will be different from this version once it has been copyedited and typeset.
PLEASE CITE THIS ARTICLE AS DOI: 10.1063/5.0102088

EDX elemental distribution analysis and XRD refinement details.

ACKNOWLEDGMENTS

Wei Xiong would like to thank the financial support of China Scholarship Council.

CRediT

Wei Xiong: Writing – Conceptualization (equal); Data curation (equal); Formal analysis (equal); Original draft (lead); Writing – review and editing (equal). **Hangfeng Zhang**: Data curation (equal); Formal analysis (equal); Supervision (equal); Writing – review and editing (equal); **Zimeng Hu:** Data curation (supporting); Investigation (supporting); **Michael J Reece:** Conceptualization (lead); Funding acquisition (lead); Formal analysis (equal); Project administration (equal); Writing – review and editing (equal). **Haixue Yan:** Conceptualization (equal); Data curation (equal); Project administration (lead); Supervision (lead); Writing – review and editing (equal).

References

(1) Rost, C. M.; Sachet, E.; Borman, T.; Moballegh, A.; Dickey, E. C.; Hou, D.; Jones, J. L.; Curtarolo, S.; Maria, J. P. Entropy-stabilized oxides. *Nature Communications* **2015**, *6*, 8485.

(2) Bérardan, D.; Franger, S.; Meena, A.; Dragoe, N. Room temperature lithium superionic conductivity in high entropy oxides. *Journal of Materials Chemistry A* **2016**, *4* (24), 9536-9541.

(3) Osenciat, N.; Bérardan, D.; Dragoe, D.; Leridon, B.; Holé, S.; Meena, A. K.; Franger, S.; Dragoe, N. Charge compensation mechanisms in Li-substituted high-entropy oxides and influence on Li superionic conductivity. *Journal of the American Ceramic Society* **2019**, *102* (10), 6156-6162.

(4) Zhai, S.; Rojas, J.; Ahlborg, N.; Lim, K.; Toney, M. F.; Jin, H.; Chueh, W. C.; Majumdar, A. The use of poly-cation oxides to lower the temperature of two-step thermochemical water splitting. *Energy & Environmental Science* **2018**, *11* (8), 2172-2178.

(5) Gild, J.; Samiee, M.; Braun, J. L.; Harrington, T.; Vega, H.; Hopkins, P. E.; Vecchio, K.; Luo, J. High-entropy fluorite oxides. *Journal of the European Ceramic Society* **2018**, *38* (10), 3578-3584.

(6) Chen, K.; Pei, X.; Tang, L.; Cheng, H.; Li, Z.; Li, C.; Zhang, X.; An, L. A five-component entropy-stabilized fluorite oxide. *Journal of the European Ceramic Society* **2018**, *38* (11), 4161-4164.

Applied Physics Letters ACCEPTED MANUSCRIPT
This is the author's peer reviewed, accepted manuscript. However, the online version of record will be different from this version once it has been copyedited and typeset.
PLEASE CITE THIS ARTICLE AS DOI: 10.1063/5.0102088
AIP Publishing

(7) Djenadic, R.; Sarkar, A.; Clemens, O.; Loho, C.; Botros, M.; Chakravadhanula, V. S. K.; Kübel, C.; Bhattacharya, S. S.; Gandhi, A. S.; Hahn, H. Multicomponent equiatomic rare earth oxides. *Materials Research Letters* **2016**, *5* (2), 102-109.
(8) Zhou, S.; Pu, Y.; Zhang, X.; Shi, Y.; Gao, Z.; Feng, Y.; Shen, G.; Wang, X.; Wang, D. High energy density, temperature stable lead-free ceramics by introducing high entropy perovskite oxide. *Chemical Engineering Journal* **2022**, *427*, 131684.
(9) Zhang, M.; Xu, X.; Ahmed, S.; Yue, Y.; Palma, M.; Svec, P.; Gao, F.; Abrahams, I.; Reece, M. J.; Yan, H. Phase transformations in an Aurivillius layer structured ferroelectric designed using the high entropy concept. *Acta Materialia* **2022**, *229*, 117815.
(10) Jiang, S.; Hu, T.; Gild, J.; Zhou, N.; Nie, J.; Qin, M.; Harrington, T.; Vecchio, K.; Luo, J. A new class of high-entropy perovskite oxides. *Scripta Materialia* **2018**, *142*, 116-120.
(11) Nguyen, T. X.; Liao, Y.-C.; Lin, C.-C.; Su, Y.-H.; Ting, J.-M. Advanced High Entropy Perovskite Oxide Electrocatalyst for Oxygen Evolution Reaction. *Advanced Functional Materials* **2021**, *31* (27), 2101632.
(12) Sharma, Y.; Musico, B. L.; Gao, X.; Hua, C.; May, A. F.; Herklotz, A.; Rastogi, A.; Mandrus, D.; Yan, J.; Lee, H. N.; et al. Single-crystal high entropy perovskite oxide epitaxial films. *Physical Review Materials* **2018**, *2* (6).
(13) Pu, Y.; Zhang, Q.; Li, R.; Chen, M.; Du, X.; Zhou, S. Dielectric properties and electrocaloric effect of high-entropy (Na0.2Bi0.2Ba0.2Sr0.2Ca0.2)TiO3 ceramic. *Applied Physics Letters* **2019**, *115* (22).
(14) Zheng, Y.; Zou, M.; Zhang, W.; Yi, D.; Lan, J.; Nan, C.-W.; Lin, Y.-H. Electrical and thermal transport behaviours of high-entropy perovskite thermoelectric oxides. *Journal of Advanced Ceramics* **2021**, *10* (2), 377-384.
(15) Banerjee, R.; Chatterjee, S.; Ranjan, M.; Bhattacharya, T.; Mukherjee, S.; Jana, S. S.; Dwivedi, A.; Maiti, T. High-Entropy Perovskites: An Emergent Class of Oxide Thermoelectrics with Ultralow Thermal Conductivity. *ACS Sustainable Chemistry & Engineering* **2020**, *8* (46), 17022-17032.
(16) Zhang, R.-Z.; Gucci, F.; Zhu, H.; Chen, K.; Reece, M. J. Data-driven design of ecofriendly thermoelectric high-entropy sulfides. *Inorganic chemistry* **2018**, *57* (20), 13027-13033.
(17) Sarkar, A.; Velasco, L.; Wang, D.; Wang, Q.; Talasila, G.; de Biasi, L.; Kubel, C.; Brezesinski, T.; Bhattacharya, S. S.; Hahn, H.; et al. High entropy oxides for reversible energy storage. *Nat Commun* **2018**, *9* (1), 3400.
(18) Xiong, W.; Zhang, H.; Cao, S.; Gao, F.; Svec, P.; Dusza, J.; Reece, M. J.; Yan, H. Low-loss high entropy relaxor-like ferroelectrics with A-site disorder. *Journal of the European Ceramic Society* **2021**, *41* (4), 2979-2985.
(19) Wang, G.; Lu, Z.; Li, Y.; Li, L.; Ji, H.; Feteira, A.; Zhou, D.; Wang, D.; Zhang, S.; Reaney, I. M. Electroceramics for High-Energy Density Capacitors: Current Status and Future Perspectives. *Chemical Reviews* **2021**, *121* (10), 6124-6172.
(20) Zhang, M.; Xu, X.; Yue, Y.; Palma, M.; Reece, M. J.; Yan, H. Multi elements substituted Aurivillius phase relaxor ferroelectrics using high entropy design concept. *Materials & Design* **2021**, *200*, 109447.

Applied Physics Letters ACCEPTED MANUSCRIPT
This is the author's peer reviewed, accepted manuscript. However, the online version of record will be different from this version once it has been copyedited and typeset.
PLEASE CITE THIS ARTICLE AS DOI: 10.1063/5.0102088

(21) Paterson, A. R.; Nagata, H.; Tan, X.; Daniels, J. E.; Hinterstein, M.; Ranjan, R.; Groszewicz, P. B.; Jo, W.; Jones, J. L. Relaxor-ferroelectric transitions: Sodium bismuth titanate derivatives. *MRS Bulletin* **2018**, *43* (8), 600-606.
(22) Wu, J.; Mahajan, A.; Riekehr, L.; Zhang, H.; Yang, B.; Meng, N.; Zhang, Z.; Yan, H. Perovskite Srx(Bi1−xNa0.97−xLi0.03)0.5TiO3 ceramics with polar nano regions for high power energy storage. *Nano Energy* **2018**, *50*, 723-732.
(23) Zhang, L.; Zhao, C.; Zheng, T.; Wu, J. Large Electrocaloric Effect in (Bi0.5Na0.5)TiO3-Based Relaxor Ferroelectrics. *ACS Applied Materials & Interfaces* **2020**, *12* (30), 33934-33940.
(24) Wang, J.-J.; Wang, Y.; Ihlefeld, J. F.; Hopkins, P. E.; Chen, L.-Q. Tunable thermal conductivity via domain structure engineering in ferroelectric thin films: A phase-field simulation. *Acta Materialia* **2016**, *111*, 220-231.
(25) Ihlefeld, J. F.; Foley, B. M.; Scrymgeour, D. A.; Michael, J. R.; McKenzie, B. B.; Medlin, D. L.; Wallace, M.; Trolier-McKinstry, S.; Hopkins, P. E. Room-Temperature Voltage Tunable Phonon Thermal Conductivity via Reconfigurable Interfaces in Ferroelectric Thin Films. *Nano Letters* **2015**, *15* (3), 1791-1795.
(26) Sarantopoulos, A.; Saha, D.; Ong, W.-l.; Magén, C.; Malen, J. A.; Rivadulla, F. Reduction of thermal conductivity in ferroelectric SrTiO3 thin films. *Physical Review Materials* **2020**, *4*, 054002.
(27) Rietveld, H. M. A Profile Refinement Method for Nuclear and Magnetic Structures. *Journal of Applied Crystallography* **1969**, *2*, 65-71.
(28) Rodriguez-Carvajal, J. Fullprof: A Program for Rietveld Refinement and Pattern Matching Analysis. In *Abstract of the Satellite Meeting on Powder Diffraction of the XV Congress of the IUCr*, Toulouse, France, 1990; p 127.
(29) Triscone, K. M. R. C. H. A. J.-M. *Physics of Ferroelectrics : A Modern Perspective*; Springer, 2007.
(30) Nakamura, E.; Mitsui, T.; Furuichi, J. A Note on the Classification of Ferroelectrics. *Journal of the Physical Society of Japan* **1963**, *18* (10), 1477-1481.
(31) Pirc, R.; Blinc, R. Vogel-Fulcher freezing in relaxor ferroelectrics. *Physical Review B* **2007**, *76* (2), 020101.
(32) Bencan, A.; Oveisi, E.; Hashemizadeh, S.; Veerapandiyan, V. K.; Hoshina, T.; Rojac, T.; Deluca, M.; Drazic, G.; Damjanovic, D. Atomic scale symmetry and polar nanoclusters in the paraelectric phase of ferroelectric materials. *Nature Communications* **2021**, *12* (1), 3509.
(33) Zhang, H.; Giddens, H.; Yue, Y.; Xu, X.; Araullo-Peters, V.; Koval, V.; Palma, M.; Abrahams, I.; Yan, H.; Hao, Y. Polar nano-clusters in nominally paraelectric ceramics demonstrating high microwave tunability for wireless communication. *Journal of the European Ceramic Society* **2020**, *40* (12), 3996-4003.
(34) Pan, H.; Li, F.; Liu, Y.; Zhang, Q.; Wang, M.; Lan, S.; Zheng, Y.; Ma, J.; Gu, L.; Shen, Y.; et al. Ultrahigh energy density lead-free dielectric films via polymorphic nanodomain design. *Science* **2019**, *365* (6453), 578-582.
(35) Chen, C.-S.; Chen, P.-Y.; Tu, C.-S. Polar nanoregions and dielectric properties in high-strain lead-free 0.93(Bi1/2Na1/2)TiO3-0.07BaTiO3 piezoelectric single crystals. *Journal of Applied Physics* **2014**, *115* (1), 014105.

Applied Physics Letters ACCEPTED MANUSCRIPT
This is the author's peer reviewed, accepted manuscript. However, the online version of record will be different from this version once it has been copyedited and typeset.
PLEASE CITE THIS ARTICLE AS DOI: 10.1063/5.0102088

(36) Miracle, D. B.; Senkov, O. N. A critical review of high entropy alloys and related concepts. *Acta Materialia* **2017**, *122*, 448-511.
(37) Chen, X.; Wang, Q.; Cheng, Z.; Zhu, M.; Zhou, H.; Jiang, P.; Zhou, L.; Xue, Q.; Yuan, F.; Zhu, J.; et al. Direct observation of chemical short-range order in a medium-entropy alloy. *Nature* **2021**, *592* (7856), 712-716.
(38) Ding, J.; Yu, Q.; Asta, M.; Ritchie, R. O. Tunable stacking fault energies by tailoring local chemical order in CrCoNi medium-entropy alloys. *Proceedings of the National Academy of Sciences* **2018**, *115* (36), 8919-8924.
(39) Ma, Y.; Wang, Q.; Li, C.; Santodonato, L. J.; Feygenson, M.; Dong, C.; Liaw, P. K. Chemical short-range orders and the induced structural transition in high-entropy alloys. *Scripta Materialia* **2018**, *144*, 64-68.
(40) Zhang, R.; Zhao, S.; Ding, J.; Chong, Y.; Jia, T.; Ophus, C.; Asta, M.; Ritchie, R. O.; Minor, A. M. Short-range order and its impact on the CrCoNi medium-entropy alloy. *Nature* **2020**, *581* (7808), 283-287.
(41) Suchanicz, J.; Czternastek, H.; Kluczewska, K.; Sitko, D.; Czaja, P.; Konieczny, K.; Nowakowska-Malczyk, M.; Węgrzyn, A. Thermal conductivity of (1-x)BaTiO3-xPb(Zn1/3Nb2/3)O3 ceramics (x = 0, 0.025, 0.05, 0.075, 0.1, 0.125 and 0.15). *Ferroelectrics* **2019**, *538* (1), 52-56.
(42) Dehkordi, A. M.; Bhattacharya, S.; Darroudi, T.; Karakaya, M.; Kucera, C.; Ballato, J.; Adebisi, R.; Gladden, J. R.; Podila, R.; Rao, A. M.; et al. Optimizing thermal conduction in bulk polycrystalline SrTiO3−δ ceramics via oxygen non-stoichiometry. *MRS Communications* **2018**, *8* (4), 1470-1476.
(43) Zhou, H. Y.; Liu, X. Q.; Zhu, X. L.; Chen, X. M. CaTiO3 linear dielectric ceramics with greatly enhanced dielectric strength and energy storage density. *Journal of the American Ceramic Society* **2018**, *101* (5), 1999-2008.
(44) Tachibana, M.; Kolodiazhnyi, T.; Takayama-Muromachi, E. Thermal conductivity of perovskite ferroelectrics. *Applied Physics Letters* **2008**, *93* (9), 092902.
(45) Suchanicz, J.; Jeżowski, A.; Poprawski, R. Low-Temperature Thermal and Dielectric Properties of Na0.5Bi0.5TiO3. *Physica Status Solidi (a)* **1998**, *169* (2), 209-215.
(46) Giri, A.; Braun, J. L.; Rost, C. M.; Hopkins, P. E. On the minimum limit to thermal conductivity of multi-atom component crystalline solid solutions based on impurity mass scattering. *Scripta Materialia* **2017**, *138*, 134-138.
(47) Callaway, J.; von Baeyer, H. C. Effect of Point Imperfections on Lattice Thermal Conductivity. *Physical Review* **1960**, *120* (4), 1149-1154.
(48) Tachibana, M.; Takayama-Muromachi, E. Thermal conductivity and heat capacity of the relaxor ferroelectric[PbMg1/3Nb2/3O3]1−x[PbTiO3]x. *Physical Review B* **2009**, *79* (10).

AIP Publishing

Applied Physics Letters ACCEPTED MANUSCRIPT

This is the author's peer reviewed, accepted manuscript. However, the online version of record will be different from this version once it has been copyedited and typeset.

PLEASE CITE THIS ARTICLE AS DOI: 10.1063/5.0102088

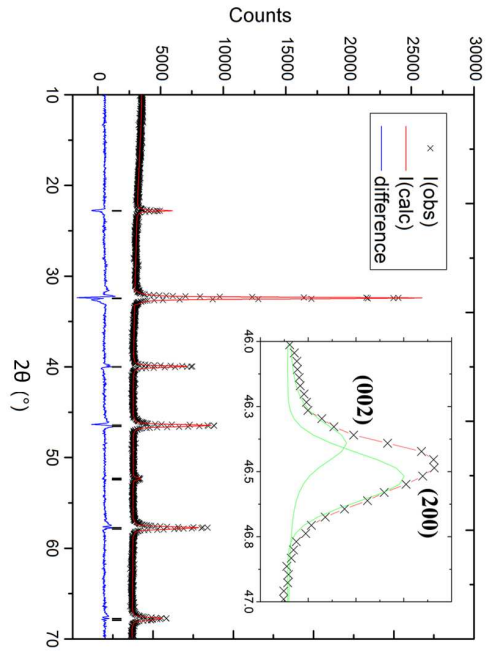

AIP Publishing

Applied Physics Letters ACCEPTED MANUSCRIPT

This is the author's peer reviewed, accepted manuscript. However, the online version of record will be different from this version once it has been copyedited and typeset.

PLEASE CITE THIS ARTICLE AS DOI: 10.1063/5.0102088

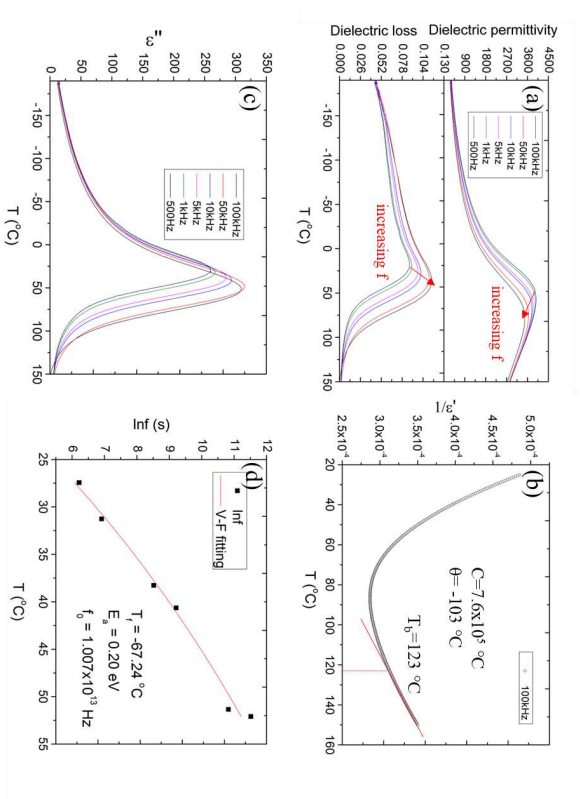

AIP Publishing

Applied Physics Letters ACCEPTED MANUSCRIPT

This is the author's peer reviewed, accepted manuscript. However, the online version of record will be different from this version once it has been copyedited and typeset.

PLEASE CITE THIS ARTICLE AS DOI: 10.1063/5.0102088

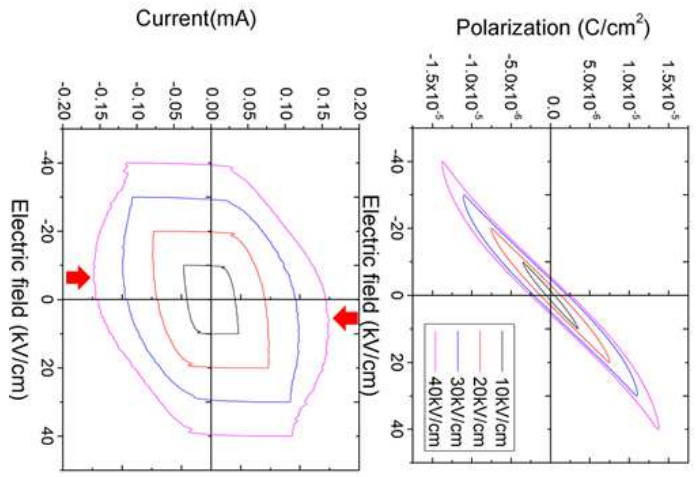

AIP Publishing

Applied Physics Letters ACCEPTED MANUSCRIPT

This is the author's peer reviewed, accepted manuscript. However, the online version of record will be different from this version once it has been copyedited and typeset.

PLEASE CITE THIS ARTICLE AS DOI: 10.1063/5.0102088